A New Species of Histiotus Gervais, 1856 (Chiroptera, Vespertilionidae), from the Pacific Coast of Northern Peru

Authors: Velazco, Paúl M., Almeida, Francisca Cunha, Cláudio, Vinícius C., Giménez, Analía L., and Giannini, Norberto P.

Source: American Museum Novitates, 2021(3979) : 1-30

Published By: American Museum of Natural History

URL: https://doi.org/10.1206/3979.1

AMERICAN MUSEUM NOVITATES

Number 3979, 30 pp. October 13, 2021

A New Species of *Histiotus* Gervais, 1856 (Chiroptera, Vespertilionidae), from the Pacific Coast of Northern Peru

PAÚL M. VELAZCO,[1] FRANCISCA CUNHA ALMEIDA,[2] VINÍCIUS C. CLÁUDIO,[3]
ANALÍA L. GIMÉNEZ,[4] AND NORBERTO P. GIANNINI[5]

ABSTRACT

The Pacific coastal desert of Peru harbors a unique bat fauna, including narrowly endemic taxa adapted to arid environments. This region was also the setting where several pre-Incan civilizations flourished. The Moche culture (100–850 CE) was one of those, with a rich and diverse material culture that included strikingly realistic ceramic representations of the regional flora and fauna. In particular, one Mochica pottery vessel is in the form of a bat that, based on external characteristics (large pinnae and tragus, pinnae connected by high band of membrane across the forehead, and lack of noseleaf), clearly represents an individual of the vespertilionid genus *Histiotus*. The morphological characteristics observed in this vessel, in addition to the area of influence of the Moche culture, suggests that this vessel depicts a species previously unknown to

---

[1] Department of Biology, Arcadia University, Glenside, PA; Division of Vertebrate Zoology (Mammalogy), American Museum of Natural History, New York.

[2] Instituto de Ecología, Genética y Evolución de Buenos Aires, Consejo Nacional de Investigaciones Científicas y Técnicas, Buenos Aires, Argentina.

[3] Instituto de Biologia, Universidade Federal de Rio de Janeiro, Rio de Janeiro, RJ, Brazil; and Center for Conservation Genomics, Smithsonian Conservation Biology Institute, Washington, DC.

[4] Centro de Investigación Esquel de Montaña y Estepa Patagónica (CIEMEP; CONICET-UNPSJB); Laboratorio de Investigaciones en Evolución y Biodiversidad (LIEB), FCNyCS, Universidad Nacional de la Patagonia San Juan Bosco, Esquel, Chubut, Argentina.

[5] Unidad Ejecutora Lillo, Tucumán, Argentina; Facultad de Ciencias Naturales e Instituto Miguel Lillo, Tucumán, Argentina; Division of Vertebrate Zoology (Mammalogy), American Museum of Natural History, New York.

ISSN 0003-0082

science that we describe here as new on the basis of two specimens obtained in 2012 in the Peruvian department of Piura. Our new species, *Histiotus mochica*, can be distinguished from other congeners by having unicolored dorsal fur, medial lobes of pinnae greater than 9.5 mm wide, and a well-developed (>4.3 mm high) transverse band of skin connecting the pinnae. Cytochrome *b* sequence data indicate that the new species is sister to *H. humboldti* from the Andes of Colombia and northern Ecuador. The new species is a medium-sized *Histiotus* that clusters with *H. laephotis*, *H. velatus*, and with small specimens of *H. montanus* in our multivariate analyses. With the description of *H. mochica*, the diversity of the genus increases to 11 species. We provide a key based on external characters of all known species of *Histiotus*.

INTRODUCTION

Vespertilionidae is the largest family of bats in the world, with about 58 genera and 509 species (Simmons and Cirranello, 2020). Vespertilionids are characterized by unadorned faces lacking a noseleaf; relatively small eyes; wing digit II reduced to the metacarpal plus a single small phalanx; and a long tail entirely enclosed within the uropatagium and reaching its distal edge (Koopman, 1994; Reid, 2009; Moratelli et al., 2019a). Eight vespertilionid genera occur in the Neotropics (*Bauerus*, *Corynorhinus*, *Eptesicus*, *Histiotus*, *Lasiurus*, *Myotis*, *Perimyotis*, and *Rhogeessa*; Gardner, 2008; Reid, 2009), but see Baird et al. (2021). In the past two decades, the taxonomy and systematics of several of these genera and their species have been the focus of numerous studies: *Corynorhinus* (e.g., Piaggio and Perkins, 2005), *Lasiurus* (e.g., Baird et al., 2015, 2017; Ziegler et al., 2016), *Myotis* (e.g., Ruedi and Mayer, 2001; Larsen et al., 2012; Moratelli et al. 2011a, 2011b, 2013), and *Rhogeessa* (e.g., Baird et al., 2008, 2012, 2019).

Bats of the genus *Histiotus* are rarely captured in the field and for that reason they are poorly represented in scientific collections, which makes them one of the least known vespertilionid genera in the Neotropics (Rodríguez-Posada, et al. 2021). *Histiotus* is endemic to South America, and its species occur in habitats along the entire length of the Andes, the Pacific coastal desert of Peru, semiarid regions of Argentina and Brazil, and the Atlantic Forest of eastern Brazil (Handley and Gardner, 2008; Semedo and Feijó, 2017; Cláudio, 2019). Bats of this genus are characterized by a greatly enlarged pinna, extending well beyond the muzzle; pinnae united by a ridge or low band of membrane across the forehead; and large tympanic bullae, so their diameter is more than twice the width between them (Miller, 1907; Handley and Gardner, 2008; Cláudio, 2019). There is some controversy regarding the taxonomic rank of *Histiotus*. Some studies treat *Histiotus* as a genus (e.g., Handley and Gardner, 2008; Rodríguez-Posada et al., 2021), whereas others consider it to be a subgenus of *Eptesicus* (e.g., Giménez et al., 2019; Simmons and Cirranello, 2020). This controversy is rooted on the fact that phylogenetic analyses of the whole Vespertilionidae family recover *Histiotus* nested within New World *Eptesicus* (Hoofer and Van Den Bussche, 2003; Roehrs et al., 2010; Amador et al., 2018). Further studies need to be performed, which might result in the recognition of several genera within what we currently recognize as *Eptesicus*. Due to the unique morphological traits of *Histiotus*, here we follow Moratelli et al. (2019a) in recognizing *Histiotus* as a distinct genus, even though this will leave *Eptesicus* paraphyletic in the interim.

The specific composition of *Histiotus* has received ample attention in the past decade (e.g., Feijó et al., 2015; Giménez et al., 2015, 2019; Rodríguez-Posada et al., 2021). From just four species recognized in 2008 (Handley and Gardner, 2008) the diversity increased to 10 with some forms still in need of formal description or revision (Rodríguez-Posada et al., 2021). The species are: *H. alienus* Thomas, 1916, known only from the type locality in southern Brazil (sometimes considered a subspecies of *H. montanus*; e.g., Handley and Gardner, 2008); *H. cadenai* Rodríguez-Posada et al., 2021, known from localities in the Central Cordillera of Colombia and northern Andes of Ecuador; *H. colombiae* Thomas, 1916, restricted to the eastern Cordillera of Colombia; *H. diaphanopterus* Feijó et al., 2015, with scattered records in central Bolivia and the central-western and northeastern regions of Brazil; *H. humboldti* Handley, 1996, known from the Andes in Venezuela, Colombia, and northern Ecuador; *H. laephotis* Thomas, 1916, known from southern Peru, Bolivia, northern Chile, eastern slope of the Andes in northwestern Argentina, western and central Paraguay, and southern Brazil; *H. macrotus* (Poeppig, 1835) known from central Chile and western Argentina; *H. magellanicus* (Philippi, 1866) known from southern Chile and Argentina; *H. montanus* (Philippi and Landbeck, 1861) known from Peru, Bolivia, Chile, Argentina, Uruguay, and south and southeastern Brazil; and *H. velatus* (I. Geoffroy St.-Hilaire, 1824) from southeastern Peru, northern Argentina and Bolivia, southern Brazil and Paraguay (Aramayo et al., 2019; Handley and Gardner, 2008; Rodríguez-Posada et al., 2021).

The Pacific coastal desert of northwestern Peru harbors a unique bat fauna, several members of which (e.g., *Amorphochilus schnablii*, *Platalina genovensium*, *Eumops wilsoni*, *Mormopterus kalinowskii*, *Myotis bakeri*, *Tomopeas ravus*) are adapted to arid environments and harsh conditions (Koopman, 1982; Ludeña and Medina, 2017; Moratelli et al. 2019b; Ossa et al., 2020; Velazco and Kline, 2019). This region also was the setting of several pre-Incan civilizations, among which was the Moche culture (CE 100–850), whose area of influence extended from the Piura valley in the north to the Nepeña Valley in the south (Alaica, 2020; Larco Hoyle, 2001; Castillo Butters and Uceda Castillo, 2008). Mochica pottery is incredibly realistic and rich in representations of the regional flora and fauna, deities interacting in myth and ritual, as well as humans performing all sorts of activities, both religious and mundane (Alaica, 2020; Larco Hoyle, 2001; Castillo Butters and Uceda Castillo, 2008). Bats were an important representation in Moche artwork (ceramics and fineline) for the link that connected its characteristics and behaviors to the adoration of the moon and to the burial ceremonies that celebrated their ancestors (Alaica, 2020). Additionally, bats were appreciated and admired for their role in the health of the ecosystems and also were considered emblems of sacrifice, with the vessels depicting their likeness capable of holding essential daily and ritual fluids (Alaica, 2020; fig. 1). One of these ceramics (fig. 1) portrays a bat that, based on external characteristics (large pinnae and tragus, pinnae connected by high band of membrane across the forehead, and lack of noseleaf), we can attest with certainty represents an individual of the genus *Histiotus*. The fact that this pottery represents a species previously unknown from this region was puzzling, but an undescribed species of *Histiotus* was recorded just a few years ago in the department of Piura in northwestern Peru (Velazco et al., 2013; Giménez et al., 2019). We believe that the Moche ceramic in question portrays this previously unknown species of *Histiotus*, which we formally describe below.

MATERIAL AND METHODS

Our study employed analyses of mitochondrial gene sequences as well as standard morphological comparisons. The specimens examined and tissues used for this study belong to the following collections:

ALP	Coleção Adriano Lúcio Peracchi, Instituto de Biologia, Universidade Federal Rural do Rio de Janeiro, Seropédica, Brazil
AMNH	American Museum of Natural History, New York
BM	The Natural History Museum, London (formerly the British Museum [Natural History], London)
CEBIOMAS	Colección de Mamíferos, Centro de Ecología y Biodiversidad, Lima, Peru
CML	Colección Mamíferos Lillo, Tucumán, Argentina
FMNH	Field Museum of Natural History, Chicago
LSUMZ	Louisiana State University Museum of Zoology, Baton Rouge, Louisiana
MACN	Museo Argentino de Ciencias Naturales, Buenos Aires
MN	Museu Nacional da Universidade Federal do Rio de Janeiro, Rio de Janeiro
MNHN ZM-MO	Muséum national d'Histoire naturelle, Paris
USNM	National Museum of Natural History (formerly the United States National Museum), Washington, D.C.

Morphological Analyses

We examined 151 specimens of adult *Histiotus* (56 males and 95 females; appendix 1) and evaluated external and osteological characters including, but not restricted to, those defined by Thomas (1916), Handley (1996), Feijó et al. (2015) and Rodríguez-Posada et al. (2021). All measurements reported herein are from adult individuals with closed epiphyses unless otherwise indicated. The first four measurements listed below were taken from skin labels or other records made by the original collector, with the exception of the ear length which was taken by us if the specimen was preserved in fluid; all other measurements were taken by us using digital calipers and were recorded to the nearest 0.01 mm. Linear measurements are given in millimeters (mm), and weights are reported in grams (g). Descriptive statistics (mean and observed range) were calculated for all samples. Measurements are defined as follows:

Total length (ToL): distance from the tip of the snout to the tip of the last caudal vertebra
Length of tail (LT): measured from the point of dorsal flexure of the tail with the sacrum to the tip of the last caudal vertebra
Hind-foot length (HF): measured from the anterior edge of the base of the calcar to the tip of the claw of the longest toe
Ear length (E):measured from the ear notch to the fleshy tip of the pinna
Width of medial lobe of ear (WMLE): maximum width of the medial lobe of the pinna (M782897)

Forearm length (F): distance from the elbow (tip of the olecranon process) to the wrist (including the carpals). This measurement is made with the wing folded
Condyloincisive length (CIL): distance from the posteriormost point on the occipital condyles to the anteriormost (mesial) point on the upper incisors
Condylocanine length (CCL): distance from the posteriormost point on the occipital condyles to the anteriormost (mesial) point on the upper canines
Postorbital breadth (PB): least breadth across the frontals posterior to the postorbital processes or bulges
Zygomatic breadth (ZB): greatest transverse dimension across the zygomatic arches
Braincase breadth (BB): greatest breadth of the globular part of the braincase
Mastoid breadth (MB): greatest cranial breadth across the mastoid region
Maxillary toothrow length (MTL): distance from the anteriormost (mesial) edge of the canine crown to the posteriormost (distal) edge of the crown of the last molar
Breadth across molars (BAM): greatest breadth between the outer edges (buccal) of the crowns of the right and left upper molars
Upper molar toothrow length (UPTL): distance from the anteriormost (mesial) edge of the M1 crown to the posteriormost (distal) edge of the crown of M3
Dentary length (DENL): distance from the midpoint of condyle to the anteriormost point of dentary
Mandibular toothrow length (MANDL): distance from the anteriormost (mesial) surface of the lower canine to the posteriormost (distal) surface of m3

All 11 craniodental measurements (CIL, CCL, PB, ZB, BB, MB, MTL, BAM, UPTL, DENL, and MANDL) and one external measurement (F) of female and male specimens were log-transformed to achieve normalization for separate multivariate analyses. Several specimens were not considered in these analyses due to missing data. We evaluated patterns of size and shape variation among taxa by principal component analysis (PCA) and discriminant function analysis (DFA). A covariance matrix was used in the PCA. Analyses were performed using PAST v4.04 (Hammer et al., 2001). We constructed a dichotomous identification key for all of the named species of *Histiotus* based on morphological traits identified during the course of the study.

Photographs of the holotype and paratype of the new species of *Histiotus* (36 images: M782861–M782896) and of other species of *Histiotus* (M782897–M782898) are available at Morphobank (http://morphobank.org/permalink/?P4025). We reference some of these images throughout our description (the image reference numbers begin with the letter M).

Molecular Analyses

The phylogenetic position of our new species among other species of the genus has been already explored (as unnamed terminal) by Giménez et al. (2019) and Rodríguez-Posada et al. (2021). We used the cyt-*b* sequences generated by the aforementioned studies to calculate the pairwise uncorrected (*p*) cyt-*b* sequence divergence within and among *Histiotus* species, and

FIGURE 1. Front (A), back (B), and lateral (C) views of a Moche ceramic vessel portraying a bat of the genus *Histiotus*. This ceramic was recovered from a Moche tomb. Several diagnostic characteristics of the genus can be observed, such as the large pinnae and tragus, pinnae connected by a band of membrane across the forehead, and lack of a noseleaf. The vessel belongs to the collections of the Cleveland Museum of Art, Cleveland, Ohio.

to determine the relationships among the different haplotypes of *Histiotus*. The molecular dataset included 2 sequences of the new species, 4 of *H. colombiae*, 4 of *H. humboldti*, 4 of *H. macrotus*, 5 of *H. magellanicus*, and 5 of *H. montanus*. We estimated the average uncorrected (*p*) pairwise distances using MEGA X (Stecher et al., 2020) and a matrix in which all sequences were trimmed to the length of the shortest sequence (767 bp). A haplotype network was obtained with the TCS method (Clement et al., 2000; Templeton et al., 1992) as implemented in the POPART software (Leigh and Bryant, 2015).

SYSTEMATICS

Family Vespertilionidae Gray, 1821

Genus *Histiotus* Gervais, 1856

Histiotus mochica, new species

Moche's leaf-eared bat

Histiotus sp.: Velazco et al. 2013: 431.
E[*ptesicus*]. (*H*[*istiotus*].) sp.: Giménez et al. 2019: 349.
Histiotus sp.: Rodríguez-Posada et al. 2021: 223.

Holotype: The holotype (CEBIOMAS 227; fig. 2A, M782861–M782887), an adult male specimen preserved in alcohol with the skull removed and cleaned, was collected by Paúl M. Velazco (original number: PMV 2478) on 21 October 2012 at the Quebrada Pariñas, 9.6 km NE of Talara (4°31′41.2″ S; 81°12′09″ W, 73 m), province of Talara, in the Peruvian department of Piura (fig. 3). Frozen tissues are deposited at the American Museum of Natural History (AMNH 278524).

Paratype: One adult female specimen (AMNH 278521; figs. 2B, 4, M782887–M782896) preserved in alcohol with the skull removed and cleaned, was collected by Paúl M. Velazco (original number: PMV 2475) on 20 October 2012 at the type locality. Frozen tissues are deposited at the American Museum of Natural History (AMNH 278521).

Distribution: *Histiotus mochica* is known only from the vicinity of the type locality in the valley of the Quebrada Pariñas (fig. 3).

Etymology: The name *mochica* honors the Moche culture. The Moche culture, also known as the Mochicas, was a regional culture in the northern coastal region of Peru and occurred between CE 100 and 850. Moche artists portrayed bats in many figurative ceramic vessels in association with themes of sacrifice, elite status, and agricultural fertility (Larco Hoyle, 2001; Alaica, 2020; fig. 1). Among the Moche people, bats were intimately intertwined with the beliefs and practices of the Moche culture and cosmology. The Moche ceramic vessel illustrated in figure 1 exhibits several diagnostic characteristics of this new species, highlighting the importance of incorporating the knowledge of present and past indigenous cultures into current research.

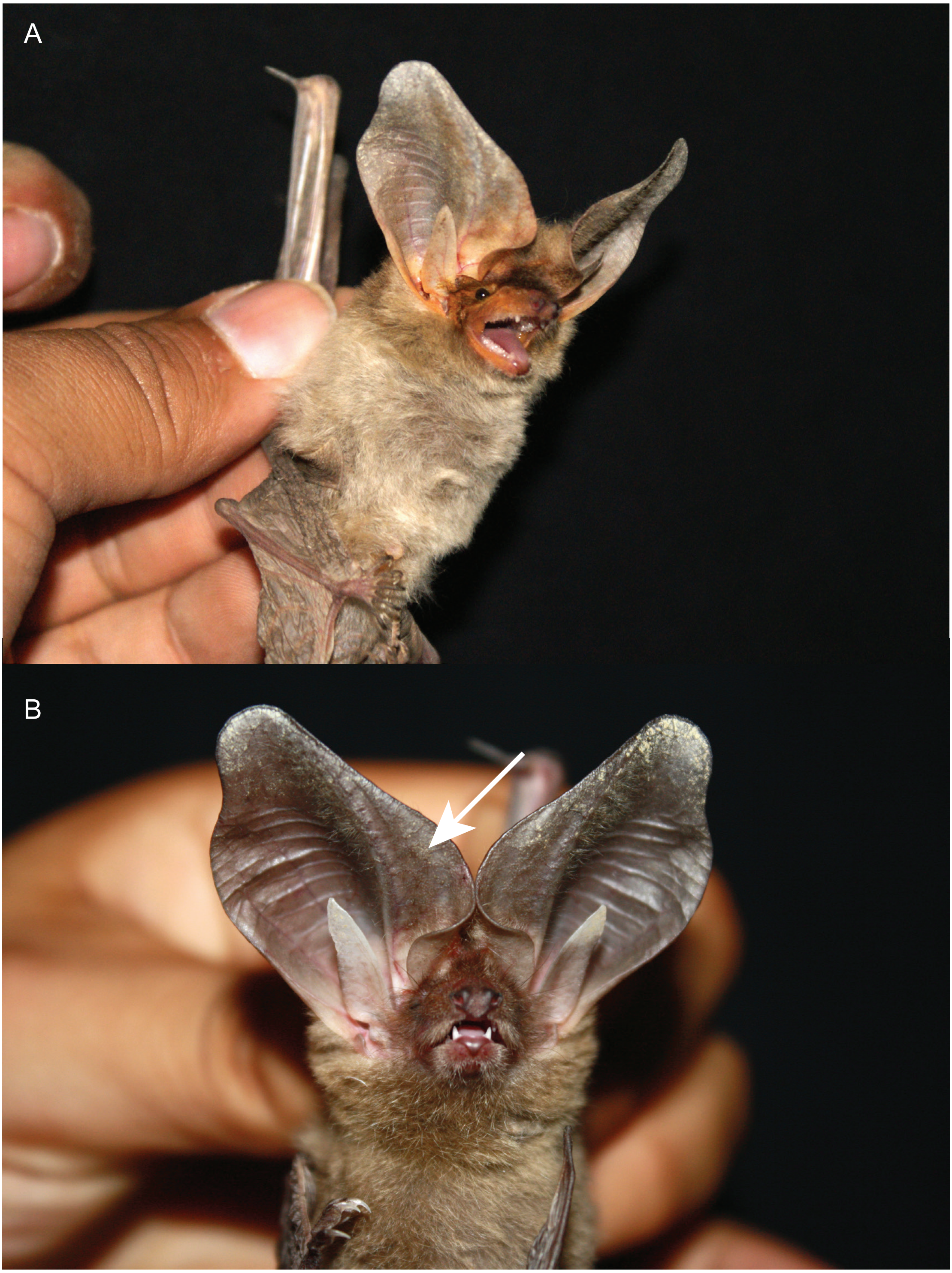

FIGURE 2. Photographs of the **A**, holotype (CEBIOMAS 227) and **B**, paratype (AMNH 278521) of *Histiotus mochica*, sp. nov. Arrow indicated the well-developed medial lobe of the pinna, diagnostic characteristic of this species.

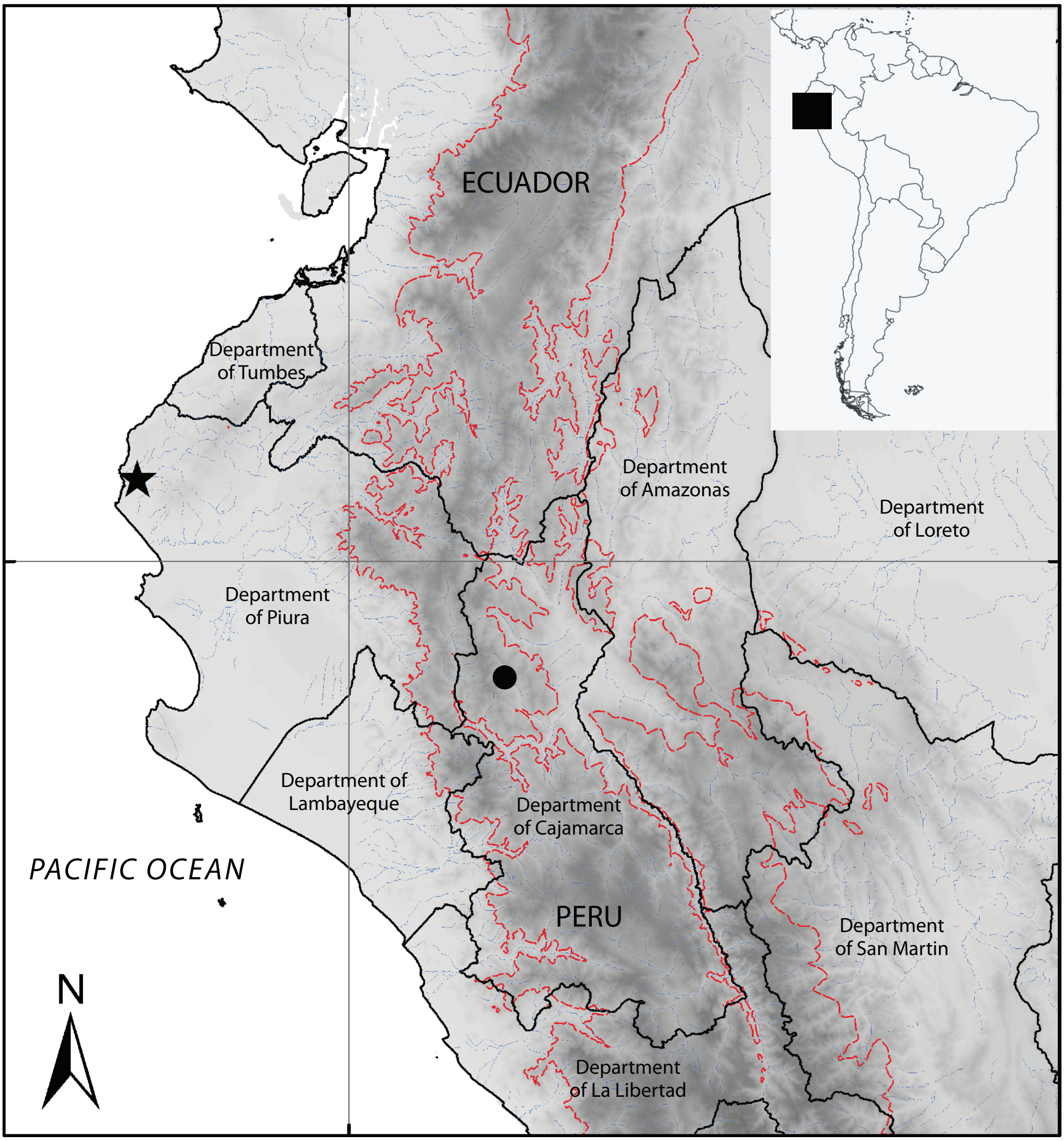

FIGURE 3. Map of southwestern Ecuador and northwestern Peru showing the type locality of *Histiotus mochica*, sp. nov. (star) and the only known locality of *Histiotus* sp. 1 (circle). Dashes red lines indicate an elevation boundary of 1500 m.

TABLE 1. Measurements (mm) and weights (g) of the type series of *Histiotus mochica*.

	Holotype CEBIOMAS 227 ♂	Paratype AMNH 278521 ♀
W	8	9.5
ToL	116	119
LT	59	60
HF	10	11.5
E	34.0	34.5
WMLE	9.7	9.8
F	46.0	47.0
CIL	16.9	17.5
CCL	15.9	16.7
PB	4.3	4.3
ZB	10.3	9.9
BB	8.6	8.0
MB	8.5	8.9
MTL	6.2	6.2
BAM	6.6	6.5
UPTL	4.0	4.1
DENL	11.7	12.1
MANDL	6.4	6.7

Diagnosis: *Histiotus mochica* is distinguished from all other species in the genus by having unicolored dorsal fur, the medial lobes of pinnae greater than 9.5 mm, and a well-developed (> 4.3 mm high) transverse band of skin connecting the pinnae (fig. 2; tables 1–3).

Description: *Histiotus mochica* is a medium-sized *Histiotus* (F 46–47 mm, CIL 16.9–17.5 mm; tables 1–3). Dorsal fur is light brown, silky, and unicolored. Ventral fur in the holotype is light brown, bicolored with lighter tips, whereas in the paratype the ventral fur is only slightly bicolored, with a similar color pattern from the observed in the holotype. The fur is long, approximately 12 mm long in hairs between the shoulders and 9 mm in hairs on the chest. Pinnae are very long (E ≥34 mm) and are connected by a well-developed (>4.3 mm high) transverse band of skin. Medial lobes of pinnae are wide (≥9.5 mm) and in contact with each other (fig. 2B). Pinnae are translucent light brown, triangular with rounded tips (fig. 2). Tragus is ensiform, with parallel edges and an acute tip (fig. 2). Patagia are translucent light brown. Plagiopatagium is attached to the metatarsal. Calcar is well developed and keeled, lacking lappets.

The skull of *Histiotus mochica* is robust, with a short rostrum and a globular braincase with a continuous slope in lateral view, and a rounded occipital border (fig. 4). The sagittal crest is weakly developed. The lambdoidal crest is well developed. The sagittal and lambdoidal crests

FIGURE 4. Dorsal and ventral views of the cranium and lateral view of the cranium and mandible of an adult female *Histiotus mochica*, sp. nov. (AMNH 278521, paratype). See table 1 for measurements. Scale bar = 5 mm.

TABLE 2. External and craniodental measurements (mm) of female individuals of *Histiotus*.

	H. alienus[1]	*H. cadenai*[2]	*H. colombiae*[3]	*H. diaphanopterus*[4]	*H. humboldti*[5]	*H. laephotis*[6]
W	–	–	15.0 (14–16) 2	10	–	11
E	27.6	–	32.8 (30.0–34.0) 8	31.0	28.8	33.9 (33.0–35.0) 5
WMLE	4.6	–	4.7 (3.6–5.4) 3	–	4.4	4.7 (4.2–5.4) 3
F	44.5	50.6	49.9 (48.7–51.4) 8	47.4	47.4	48.3 (47.3–49.9) 5
CIL	17.0	17.1	17.5 (17.1–17.7) 5	17.2	16.3	17.3 (17.0–17.7) 3
CCL	16.0	16.4	16.6 (16.2–16.9) 5	16.5	15.4	16.4 (16.2–16.7) 3
PB	4.5	4.6	4.7 (4.5–4.9) 9	3.8	4.7	4.2 (4.0–4.4) 4
ZB	11.2	–	10.9 (10.4–11.5) 6	10.4	9.8	10.7 (10.7–10.9) 3
BB	8.3	8.4	8.6 (8.2–8.9) 7	7.6	8.4	8.1 (8.0–8.3) 3
MB	9.1	9.1	9.4 (9.0–9.7) 7	8.8	8.9	9.4 (9.2–9.5) 3
MTL	6.4	6.1	6.5 (6.1–6.7) 9	6.1	5.9	6.2 (6.0–6.5) 4
BAM	7.1	6.5	7.1 (6.6–7.5) 9	6.4	6.3	6.8 (6.6–7.0) 4
UPTL	4.2	4.0	4.2 (4.0–4.3) 9	4.1	3.7	4.1 (4.0–4.2) 4
DENL	12.1	12.5	12.7 (12.3–13.3) 8	12.5	11.6	12.8 (12.3–13.0) 4
MANDL	6.9	6.6	6.9 (6.6–7.1) 9	6.6	6.2	6.7 (6.5–7.0) 4

	H. macrotus[7]	*H. magellanicus*[8]	*H. montanus*[9]	*H. velatus*[10]	*Histiotus* sp. 1[11]
W	13.3 (11.0–16.0) 5	15.4 (13.0–16.0) 5	10.5 (9.0–12.0) 2	–	10
E	34.2 (26.0–39.1) 13	24.5 (20.0–29.0) 12	27.1 (22.0–36.0) 18	28.0 (25.0–31.0) 29	29.0
WMLE	5.8 (5.1–6.2) 8	3.1 (3.0–3.2) 2	4.2 (3.7–4.7) 5	7.8 (7.2–8.3) 15	3.8
F	50.6 (46.5–53.3) 13	47.0 (45.7–48.2) 11	47.2 (44.4–51.7) 18	47.4 (44.5–50.2) 31	46.9
CIL	18.2 (17.5–19.1) 10	17.8 (17.6–18.3) 11	17.3 (16.8–17.9) 14	17.2 (16.3–18.2) 25	16.4
CCL	17.4 (16.5–18.2) 10	16.9 (16.6–17.5) 11	16.5 (16.1–17.0) 14	16.3 (15.5–17.3) 25	15.8
PB	4.6 (4.3–4.9) 11	4.7 (4.4–5.2) 11	4.3 (3.9–4.6) 17	4.1 (3.8–4.5) 28	4.9
ZB	11.4 (10.5–12.1) 11	11.6 (11.0–12.2) 11	11.2 (10.1–12.0) 15	10.5 (9.6–11.2) 27	10.6
BB	8.6 (8.2–9.3) 11	8.6 (8.4–9.0) 11	8.2 (7.9–8.5) 15	8.0 (7.6–8.2) 28	8.3
MB	9.7 (9.3–10.2) 10	9.6 (9.3–10.0) 11	9.2 (9.0–9.6) 13	9.0 (8.6–9.4) 27	8.9
MTL	6.7 (6.0–7.1) 11	6.8 (6.6–7.1) 11	6.4 (5.9–6.7) 16	6.1 (5.6–6.7) 28	6.2
BAM	7.2 (6.7–7.6) 11	7.5 (6.9–7.8) 11	7.0 (6.2–7.6) 16	6.6 (5.8–7.0) 27	6.8
UPTL	4.4 (4.0–4.6) 11	4.4 (4.2–4.7) 11	4.2 (3.8–4.5) 16	4.0 (3.8–4.3) 29	4.1
DENL	13.4 (12.5–14.2) 11	13.5 (13.2–14.1) 11	12.8 (11.6–13.4) 16	12.6 (12.0–13.4) 29	11.9
MANDL	7.2 (6.7–7.6) 11	7.2 (7.0–7.5) 11	6.9 (6.3–7.3) 16	6.5 (6.1–7.0) 29	6.7

[1] BM 1909.11.19.1.

[2] AMNH 67648.s

[3] Summary statistics (mean, observed range in parentheses, and sample size) for measurements of BM 1899.11.4.1; FMNH 72170–72174; MNHN-ZM-MO 1904-1179; USNM 513495–513496.

[4] AMNH 264086.

[5] MNHN-ZM-MO 1972-762.

[6] Summary statistics (mean, observed range in parentheses, and sample size) for measurements of BM 1897.2.25.4, 1902.1.5.1, 1934.9.2.20; CML 6103; MACN 16814.

[7] Summary statistics (mean, observed range in parentheses, and sample size) for measurements of BM 1935.11.10.13, 1935.11.10.14, 1935.11.10.16, 1935.11.10.17, 1935.11.10.18, 1935.11.10.19; CML 5406, 6061, 7894, 9884; LSUMZ 16784; USNM 391787–391788.

[8] Summary statistics (mean, observed range in parentheses, and sample size) for measurements of AMNH 93314; BM 1907.4.5.1, 1908.3.1.1; CML 3231, 10853; FMNH 23619–23621, 23623, 127477–127479.

[9] Summary statistics (mean, observed range in parentheses, and sample size) for measurements of AMNH 37194, 183876, 188780–188781; BM 1916.1.6.1, 1916.1.6.2; CML 5568; FMNH 50780–50781, 65634–65635, 75149; MACN 13844, 16809, 16815, 23650; MNHN-ZM-MO 1874-53; USNM 391789, 548682.

[10] Summary statistics (mean, observed range in parentheses, and sample size) for measurements of ALP 1522, 1579, 1581, 2096, 2350, 4845, 4942, 5088, 5595; AMNH 217565, 243887; BM 1903.7.7.17; FMNH 26466, 66389, 66391, 66393, 68497–68499, 68501–68502, 68506; MACN 16808, 18054, 18056, 18058; MN 23049, 23071–23072; USNM 105589, 548683.

[11] AMNH 268090.

do not intersect, and the triangular plate formed in some species at the intersections of the sagittal and lambdoidal crests is absent. The parietals are highly convergent toward the anterior region of the braincase, forming a conspicuous constriction at the posterior end of the rostrum (fig. 4). The rostrum is narrow with an anterior, moderate (as compared with other vespertilionids) palatal emargination. The supraorbital region is not swollen, without marked postorbital ridges. The palate is vaulted. The distance between the posterior edge of M3 and the medial edge of the posterior border of the palate is 2.5 mm. The ectotympanic and cochlea are large (fig. 4). The paracondylar process is wide and well developed. The angular process of the mandible is well developed and is projected more posteriorly than the condyloid process in lateral view (fig. 4).

Like other species in the genus, *Histiotus mochica* has a dental formula of I2/3, C1/1, P1/2, M3/3 = 32 teeth (fig. 4). The upper inner incisor (I1) is bicuspidate, with the medial cusp larger than the distal cusp. The I1 are slanted medially. Both cusps on I1 are arranged at an obtuse angle relative to the long axis of the toothrow (fig. 4). The second upper incisor (I2) is unicuspidate and smaller than I1. The first and second upper incisors are in contact and are separated from the canine by a large diastema (fig. 4). The upper toothrow is straight. The single upper premolar is triangular in occlusal view and presents wide lingual and labial cingula; it lacks an anterior projection. M1 and M2 are subequal in size (fig. 4). The labial cingula in M1 and M2 are discontinuous at the level of the mesostyle. The metacones of M1 and M2 are taller than their paracones. In M3 the metacone is poorly developed and shorter than the paracone. The protocones of M1–M3 are well developed but blunt. A parastyle is present and well developed on all upper molars. The metastyle is well developed on M1 and M2. M3 lacks a metastyle (fig. 4). The preparacrista is shorter than the postparacrista on M1 and M2, but the preparacrista is longer than the postparacrista on M3 (fig. 4). The premetacrista is shorter than the postmetacrista on M1 and M2, but the postmetacrista is absent on M3 (fig. 4).

The three lower incisors are tricuspidate and similar in size. The second and third lower incisor have a small accessory cusp on the lingual side. The lower canine has a mesiolingual cusp. The first lower premolar is shorter than the second lower premolar. Both lower premolars are bounded by well-developed cingulids. The lower molars (m1, m2, and m3) are similar in shape. The m3 is slightly shorter in anteroposterior length than m1 and m2. The protoconids are taller than the hypoconids on all three lower molars. The m1 and m2 have each a well-developed hypoconulid; m3 lacks a hypoconulid. The cristid obliqua contacts the protocristid on m1 and m2, but not the one on m3.

COMPARISONS: *Histiotus mochica* can be easily distinguished from all other species of the genus by a combination of external characters. The dorsal hairs are unicolored in *H. mochica*, whereas all the other species of the genus have dorsal bicolored hairs. The medial lobes of pinnae are greater than 9.5 mm in *H. mochica* and *H. diaphanopterus*, whereas all the other species have narrower medial lobes. The transverse band of skin connecting the pinnae is well developed (>4.3 mm high), whereas all the other species in the genus have a shallower transverse band. All the other differences among the *Histiotus* species are summarized in table 4. There

TABLE 3. External and craniodental measurements (mm) of male individuals of *Histiotus*.

	H. colombiae[1]	*H. humboldti*[2]	*H. laephotis*[3]	*H. macrotus*[4]	*H. magellanicus*[5]	*H. montanus*[6]	*H. velatus*[7]
W	–	–	10.3 (9–11) 4	10.8 (10.0–11.5) 2	12.2 (10.5–15.0) 3	10.5 (8.0–13.0) 2	–
E	32.8 (32.0–33.0) 5	27.4 (25.4–29.1) 3	32.4 (28.0–36.0) 13	33.0 (27.6–35.8) 8	26.0 (23.0–30.0) 5	28.5 (23.3.–38.0) 8	27.1 (23.5–30.2) 13
WMLE	–	4.8 (4.5–5.1) 3	5.4 (4.2–6.6) 5	6.0 (5.4–7.0) 6	–	4.4 (4.1–4.8) 3	6.9 (5.7–8.0) 6
F	47.9 (46.5–48.9) 5	46.0 (45.4–46.9) 3	47.0 (44.4–49.0) 13	49.7 (47.0–51.8) 8	46.0 (44.8–47.87) 5	47.6 (45.6–50.0) 8	46.9 (44.7–49.0) 13
CIL	17.1 (16.9–17.3) 3	15.9 (15.6–16.5) 3	17.0 (16.6–17.7) 8	17.9 (16.8–18.9) 6	17.3 (16.6–17.9) 4	17.1 (16.8–17.5) 6	17.1 (16.4–17.8) 8
CCL	16.3 (16.1–16.5) 3	15.2 (14.7–15.7) 3	16.1 (15.7–16.9) 9	17.1 (16.0–18.0) 6	16.4 (15.8–17.0) 4	16.3 (16.0–16.7) 6	16.2 (15.5–17.0) 8
PB	4.7 (4.6–4.8) 5	4.5 (4.5–4.6) 3	4.3 (4.0–4.5) 10	4.7 (4.5–4.9) 6	4.5 (4.4–4.6) 4	4.5 (4.1–4.9) 8	4.0 (3.8–4.3) 9
ZB	10.9 (10.7–11.1) 3	9.4 (9.2–9.6) 3	10.5 (10.2–10.9) 8	11.4 (11.0–11.8) 6	11.6 (11.4–12.0) 3	10.8 (10.0–11.5) 7	10.5 (9.9–11.0) 8
BB	8.6 (8.4–8.8) 4	8.0 (7.9–8.2) 3	8.1 (7.9–8.5) 10	8.6 (8.2–8.9) 6	8.5 (8.3–8.6) 5	8.3 (8.0–8.7) 7	8.0 (7.8–8.4) 8
MB	9.3 (9.1–9.6) 3	8.7 (8.5–9.0) 3	9.0 (8.6–9.5) 10	9.5 (8.9–9.9) 6	9.3 (8.7–9.6) 5	9.0 (8.8–9.3) 6	8.8 (8.2–9.2) 8
MTL	6.4 (6.3–6.5) 5	5.6 (5.5–5.7) 3	6.0 (5.8–6.2) 11	6.7 (6.3–6.9) 6	6.6 (6.2–7.0) 5	6.4 (6.0–6.8) 8	6.0 (5.7–6.3) 11
BAM	7.0 (6.8–7.2) 4	6.1 (6.1–6.2) 3	6.6 (6.4–6.9) 10	7.4 (7.1–7.6) 6	7.1 (6.6–7.6) 4	6.8 (6.2–7.1) 8	6.5 (6.1–7.0) 10
UPTL	4.1 (4.1–4.3) 5	3.6 (3.6–3.7) 3	4.0 (3.9–4.3) 10	4.4 (4.3–4.6) 6	4.3 (4.1–4.5) 5	4.2 (4.1–4.3) 8	4.0 (3.8–4.2) 11
DENL	12.6 (12.2–13.1) 5	11.4 (11.0–11.7) 3	12.2 (11.6–13.2) 11	13.4 (12.6–14.0) 6	13.1 (12.2–13.6) 5	12.7 (12.3–13.4) 8	12.5 (11.6–13.4) 11
MANDL	6.9 (6.8–7.0) 5	5.9 (5.8–6.0) 3	6.5 (6.3–6.7) 11	7.1 (6.7–7.3) 6	7.2 (6.8–7.4) 5	6.8 (6.3–7.5) 8	6.5 (6.0–6.8) 11

[1] Summary statistics (mean, observed range in parentheses, and sample size) for measurements of FMNH 72165–72169.

[2] Summary statistics (mean, observed range in parentheses, and sample size) for measurements of USNM 370967, 370970, 560627.

[3] Summary statistics (mean, observed range in parentheses, and sample size) for measurements of AMNH 181527–181528; BM 1897.2.25.1, 1904.10.2.1, 1934.11.4.1, 1934.11.4.2, 1938.9.26.3; CML 4515, 5253, 7058, 10833; MACN 16810, 16811.

[4] Summary statistics (mean, observed range in parentheses, and sample size) for measurements of BM 1935.11.10.1, 1935.11.10.3, 1935.11.10.4, 1935.11.10.5, 1935.11.10.6; CML 6059, 6185; MNHN-ZM-MO 1999-962.

[5] Summary statistics (mean, observed range in parentheses, and sample size) for measurements of CML 9887, 10854; FMNH 23622, 23624, 127480.

[6] Summary statistics (mean, observed range in parentheses, and sample size) for measurements of BM 1903.7.3.2, 1904.10.2.2, 1928.12.11.1; CML 1758; LSUMZ 19215, 27260; MACN 16505, 16813.

[7] Summary statistics (mean, observed range in parentheses, and sample size) for measurements of ALP 2349; FMNH 68496, 68504; MACN 16812, 18053, 18055, 18057, 18059; MN 3547, 6516; MNHN-ZM-MO 1999-963; USNM 391142, 548684.

TABLE 4. Morphological differences among species of *Histiotus*.

Species	Dorsal fur	Ventral fur	Ear shape	Ear color	Pinnae separation[1]	Medial lobe width (mm)	Transverse band height (mm)[2]	Patagia color
H. alienus	Bicolored	Bicolored	Slightly triangular	Dark grey	Separated	4.6	<1.0	Dark grey
H. cadenai	Bicolored	Bicolored	Triangular	Dark brown	Separated	4.8	Absent	Dark brown
H. colombiae	Bicolored	Bicolored	Oval or slightly triangular	Dark brown	Separated	3.5–5.0	Absent	Dark brown
H. diaphanopterus	Bicolored	Bicolored	Triangular	Translucent brown	Joint	9.8–12.6[3]	≅4.0	Translucent brown
H. humboldti	Bicolored	Bicolored	Slightly triangular	Brown	Joint	4.4–5.1	1.0–2.0	Light brown
H. laephotis	Bicolored	Bicolored	Slightly triangular	Dark brown	Joint	4.2–6.6	1.0–2.5	Translucent brown
H. macrotus	Bicolored	Bicolored	Slightly triangular	Brown	Joint	5.0–7.0	1.0–3.0	Brown
H. magellanicus	Bicolored	Bicolored	Oval	Dark brown	Separated	3.0–3.2	Absent	Dark brown
H. mochica	Unicolored	Unicolored/ bicolored	Triangular	Translucent brown	Joint	9.7–9.8	4.4–4.9	Translucent brown
H. montanus	Bicolored	Bicolored	Oval	Brown	Separated	3.7–4.8	0.5–1.0	Brown/ translucent brown
H. velatus	Bicolored	Bicolored	Triangular	Brown	Joint	5.7–8.3	2.0–4.0	Light to dark brown

[1] For examples of the different conditions see figure 2B (joint, *H. mochica*) and M782898 (separated, *H. montanus*).
[2] The band may be higher close to the pinna, and low or absent at the midline. The measures reported here were at the midline of the band.
[3] Feijó et al. (2015).

are no diagnostic cranial or dental characteristics that separate *H. mochica* from the other species of the genus. All the characteristics we examined were variable when multiple specimens of the same species were examined.

The nearest record of another *Histiotus* species to the type locality of *H. mochica* is a record of an unnamed taxa (AMNH 268090) from the department of Cajamarca in Peru (fig. 3). This record was reported as distinct by Rodríguez-Posada et al. (2021) as *Histiotus* sp. Here we identify this individual as *Histiotus* sp. 1. *H. mochica* can be easily distinguished from *Histiotus* sp. 1 by: dorsal unicolored hairs (bicolored in *Histiotus* sp. 1), medial lobes of pinnae greater than 9.5 mm (3.8 mm in *Histiotus* sp. 1), pinnae translucent brown and in contact medially (dark brown and separated in *Histiotus* sp. 1), transverse band of skin connecting the pinnae high >4.3 mm (band absent in *Histiotus* sp. 1), translucent brown patagia (brown in *Histiotus* sp. 1), triangular plate formed at the intersections of the sagittal and lambdoidal crests absent (weakly developed in *Histiotus* sp. 1), narrow rostrum (bulbous and wide in *Histiotus* sp. 1), and the distance between the posterior edge of M3 and the medial edge of the posterior border of the palate is 2.5 mm (<2.5 mm in *Histiotus* sp. 1).

Morphometric Analyses: Multivariate analyses included the measurements of 103 specimens of *Histiotus*, including one each of *H. alienus*, *H. cadenai*, *H. diaphanopterus*, and *Histiotus* sp. 1, 6 of *H. colombiae*, 4 of *H. humboldti*, 11 of *H. laephotis*, 15 of *H. macrotus*, 14 of *H. magellanicus*, 2 of *H. mochica*, 18 of *H. montanus*, and 29 of *H. velatus* (appendix 1).

The first two principal components accounted for 83.6% of total variance in the log-transformed measurements of this material (appendix 2). The first principal component (PC1) accounted for 69.7% of the total variation; having uniformly positive scores, PC1 represents an axis strongly influenced by size based on character loadings (figs. 5A and 5B, appendix 2). Size differences are also evidenced on the plot of PC1, with different size-related clusters distributed along the axis; at the left portion, specimens of small-bodied species (e.g., *H. humboldti* and *H. velatus*) have low scores, large-bodied species (e.g., *H. macrotus* and *H. magellanicus*) have high scores, and medium-sized species (e.g., *H. alienus*, *H. colombiae*, *H. montanus*) have intermediate values (fig. 5A). *H. mochica* cluster with *H. laephotis*, *H. velatus*, and the smaller specimens of *H. montanus* along the PC1 axis (fig. 5A). PC2 accounted for 13.8% of the total variation, and all the species, except for *H. humboldti*, extensively overlap along this axis. The PC2 correlations of the measurements PB and BB contrast with mandible length measurements (DENL and MANDL), suggesting some degree of shape differentiation among the species; however, general results highlight the skull resemblance between species of *Histiotus*.

The pattern observed in the discriminant analysis is similar to that observed in the principal component analysis. The first two discriminant functions (DF1 and DF2) summarized 83.6% of the total variation in the log-transformed measurements of the material (fig. 6, appendix 2). The first discriminant function (DF1) accounted for 58.7% of the total variation; having uniformly positive scores, DF1 also is related to size, with scores similar to the observed in PC1 (fig. 6). The confusion matrix classified correctly both individuals of *H. mochica*; however, the analysis also classified one male (AMNH 181528) *H. laephotis* as *H. mochica* (appendix 3).

Molecular Analyses: The description of *Histiotus mochica* increases to 11 the number of species in the genus. The most up-to-date phylogenetic analysis of the genus includes only six species (Rodríguez-Posada et al., 2021: fig. 2). *H. alienus*, *H. cadenai*, *H. diaphanopterus*, *H. laephotis*, and *H. velatus* are yet to be included in a phylogenetic analysis. Rodríguez-Posada et al. (2021, fig. 2) recovered a sister relationship between *H. mochica* and *H. humboldti*. The mean genetic distance between these two species is 3.2% (appendix 4).

The haplotype network (fig. 7) confirmed the distinctiveness of *H. colombiae* and *H. magellanicus*, which were separated from the other *Histiotus* species by the largest number of substitutions. It also confirmed the low diversity previously found among *H. macrotus* and *H. montanus* specimens from Chubut, Argentina, showing that these species share at least one cyt-*b* haplotype in that region. *H. humboldti* haplotypes were the most similar to the single haplotype found in the two specimens of *H. mochica* analyzed herein. *H. humboldti* and *H. mochica* haplotypes differed in at least 20 substitutions.

Natural History: The habitat at type locality, Quebrada Pariñas, is classified as a wooded savanna characterized by the following tree species: *Prosopis pallida* (Fabacea), *Acacia macracantha* (Fabacea), *Parkinsonia aculeata* (Fabaceae), *Colicodendron scabridum*

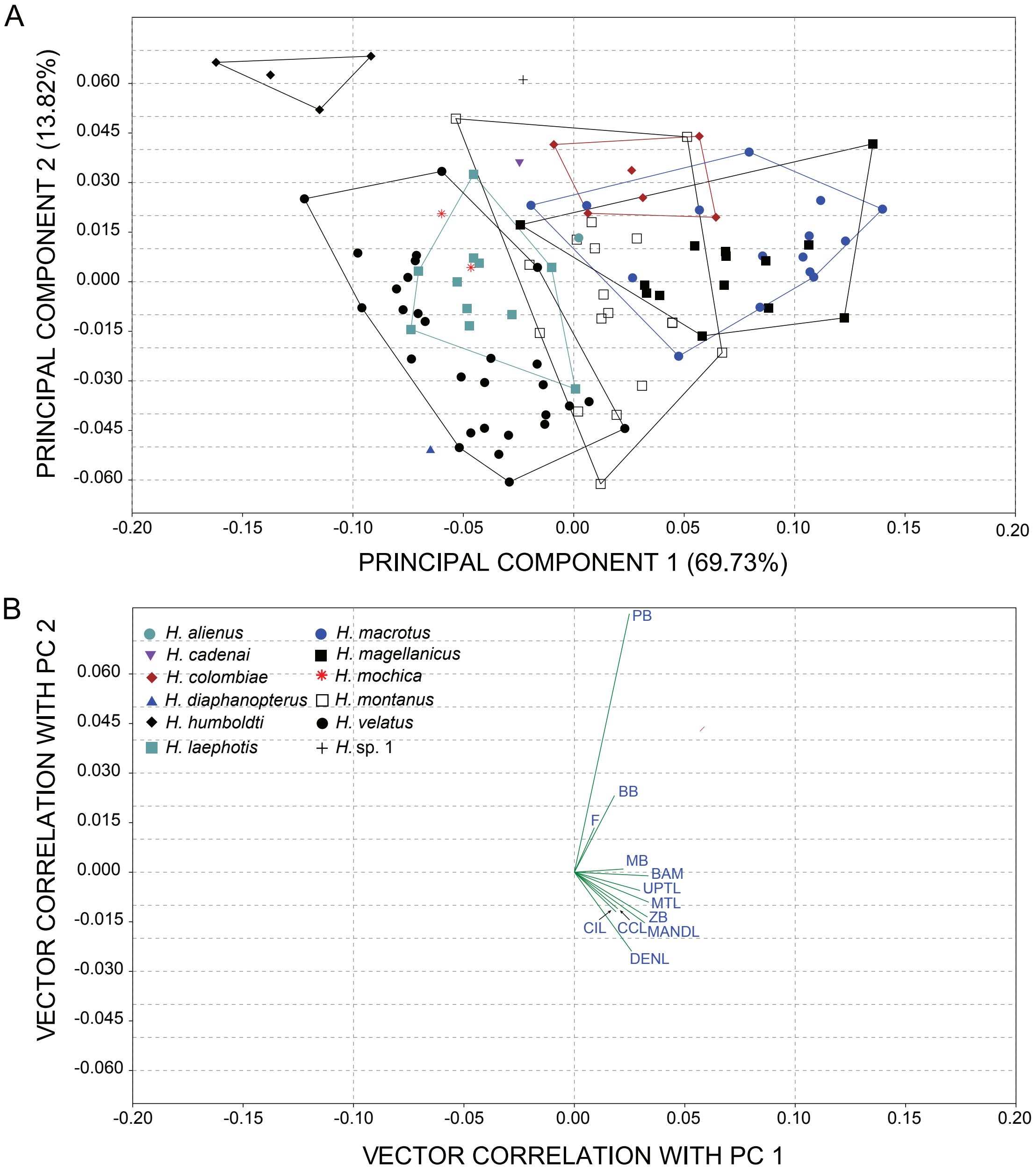

FIGURE 5. Results of principal components analysis. Plots of multivariate individual scores in the **A**, first two principal components and the **B**, corresponding vector correlations for one external and 11 craniodental characters with the first two eigenvectors of the principal components. Symbol legends for the different taxa shown in A are shown in B. See text for explanation and appendix 2 for factor loadings and other results.

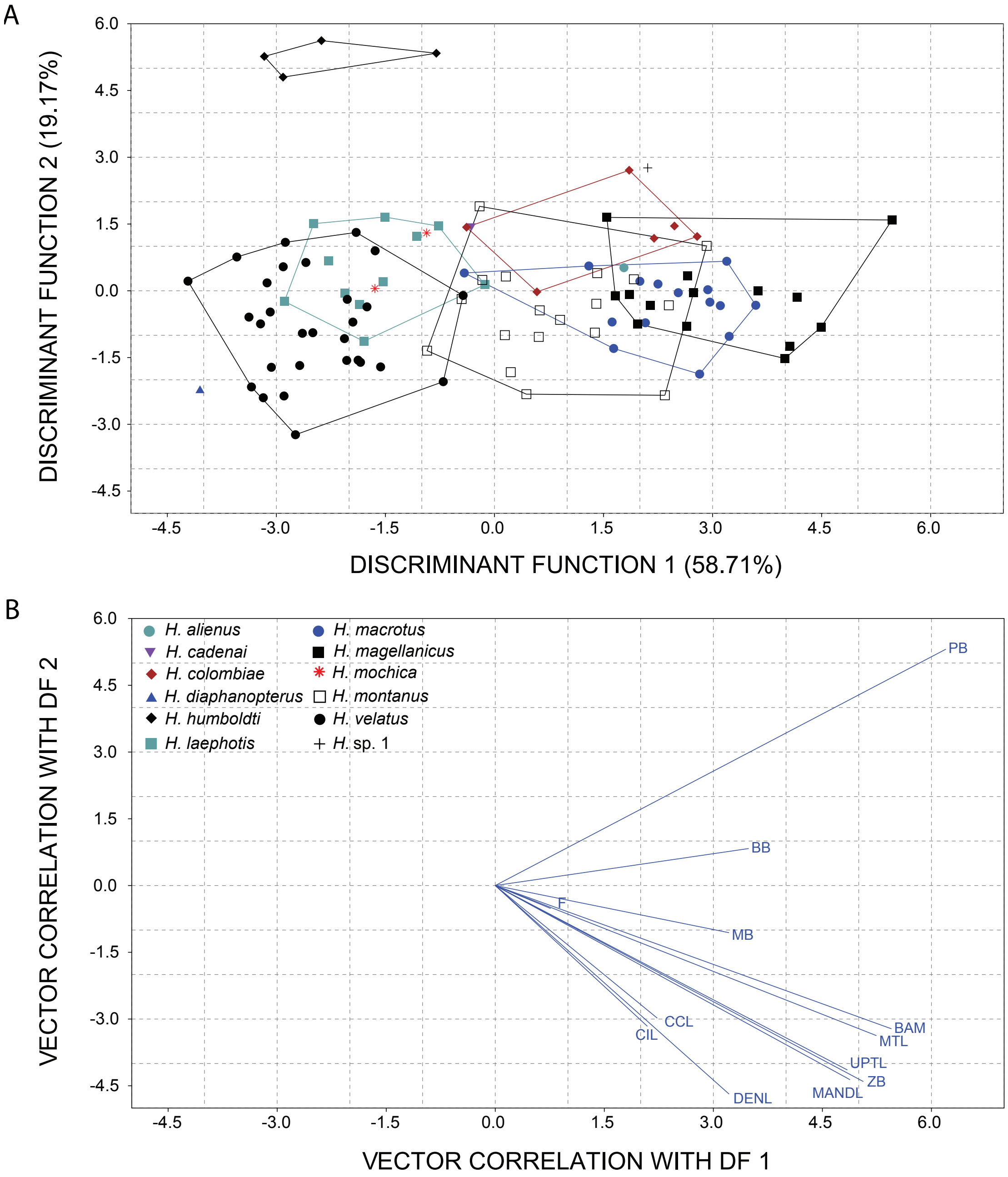

FIGURE 6. Results of discriminant function analysis. Plots of multivariate individual scores in the **A**, first two discriminant functions and the **B**, corresponding vector correlations for one external and 11 craniodental characters with the first two eigenvectors of the discriminant functions. Symbol legends for the different taxa shown in A are shown in B. See text for explanation and appendix 2 for factor loadings and other results.

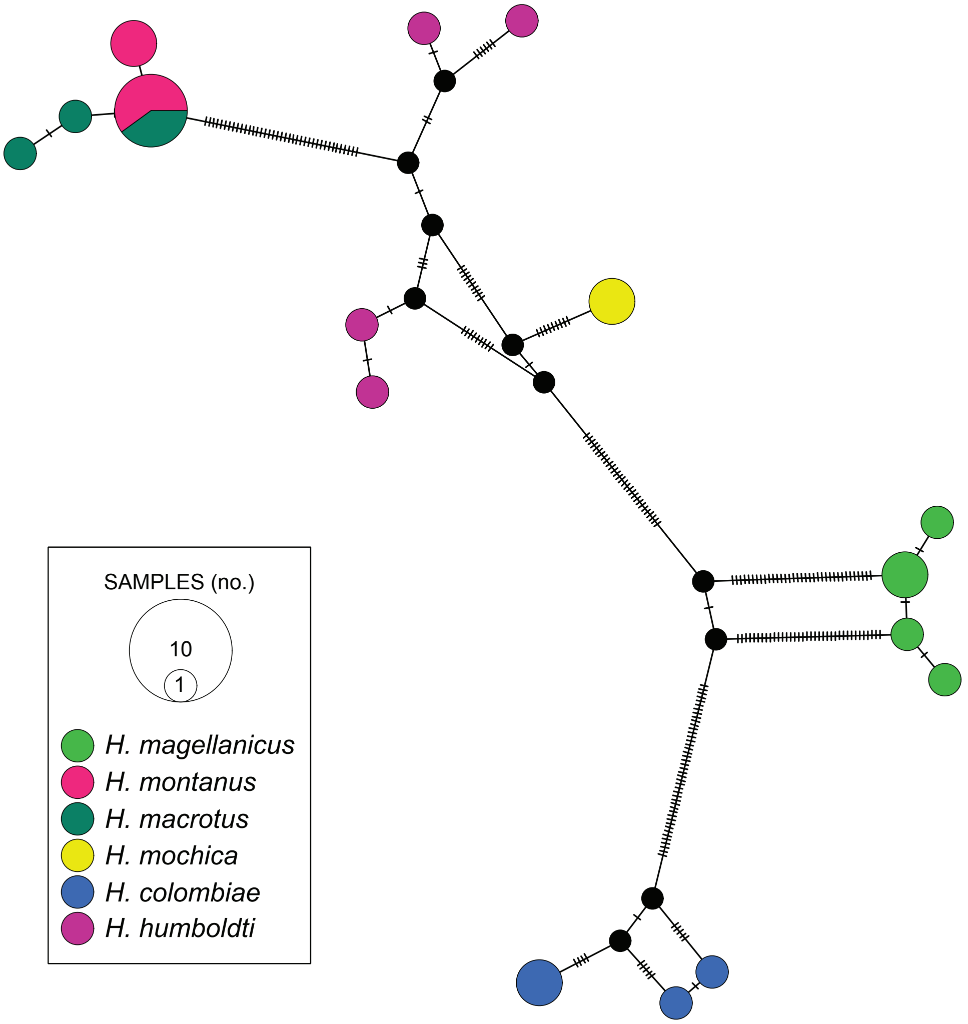

FIGURE 7. Haplotype network of the cytochrome *b* gene obtained with the TCS method. Colored circles represent different observed haplotypes; samples of different species appear in different colors and the circle size is proportional to haplotype frequency. Dashes cutting the edges represent nucleotide substitutions.

(Capparacea), *Capparis avicennifolia* (Capparacea), and by the extremely abundant introduced *Casuarina equisetifolia* (Casuarinaceae) (Velazco et al., 2013, 2014; figs. 3, 8). The two specimens of *Histiotus mochica*, were captured in consecutive days using ground level mist nets. On October 20, 2012, the now designated paratype (AMNH 278521; fig. 2B, 4) was captured at 19:00 hr together with one male adult *Myotis albescens* (CEBIOMAS 225) and one male adult *Tomopeas ravus* (CEBIOMAS 226; Velazco et al., 2013, fig. 4). The holotype (CEBIOMAS 227; fig. 2A) was captured on October 21, 2012, at 19:00 hr using the same mistnet that captured the paratype the day before. Along with the holotype, we captured one male adult *Myotis albescens* (AMNH 278526), one male adult *Tomopeas ravus* (AMNH 278525; Velazco et al., 2013, fig. 2 [right]), and one *Glossophaga soricina* with a pup that were released.

DISCUSSION

With the description of *Histiotus mochica*, the genus *Histiotus* now includes 11 species, all endemic to South America. The type locality of *H. mochica* falls within Koopman's (1982) zoogeographical area "Pacific coast of Peru and northern Chile." This area harbors one of the most unique bat faunas in all South America (Koopman, 1982). While the diversity is not high (25 species), this region contains the highest percentage (32%) of endemic bat species among all South American areas (e.g., *Amorphochilus schnablii*, *Platalina genovensium*, *Myotis bakeri*, etc.). The high rate of anthropogenic disturbances (i.e., agriculture, urban expansion, mining, deforestation, and other anthropogenic factors) in the region, especially in northern Peru, threatens this amazing diversity (Velazco et al., 2013). However, one such threat might be contributing to the conservation of the bat fauna in the region. The Pacific coast of northern Peru is rich in oil deposits: several oil-concession lands there have limited access to people and restricted opportunities for land development, indirectly affording protection to bats in those areas (Velazco et al., 2013).

Gloger's rule is an ecogeographical rule that connects an animal's coloration with the climatic variation in their home range (i.e., animals seemed more pigmented in tropical regions) (Rensch, 1929, 1936). Gloger's rule can be defined in two ways: (1) a simple version that predicts either the increased of overall melanin deposition in warm and humid climates or the decrease of overall melanin deposition in cold and wet climates or (2) a complex version that treats temperature and humidity effects on both main types of melanin (eumelanin and phaeomelanin) deposited in animals independently (Delhey, 2019). The lighter coloration of the pelage and patagia of *Histiotus mochica* seems to fit one of the complex rules that states that in dry environments the deposition of eumelanin decreases while the deposition of phaeomelanin increases. However, the quantification of these pigments requires analyses (e.g., high-performance liquid chromatography [HPLC] with UV detection) that are beyond the scope of our study (Affenzeller et al., 2019).

The taxonomy of *Histiotus* has changed drastically in recent years (Cláudio, 2019). Since the compilations of Simmons (2005), who recognized seven species, and Handley and Gardner

FIGURE 8. Overview of the Quebrada Pariñas in October 2012 where the two specimens of *Histiotus mochica* were captured.

(2008), who recognized only four species in the genus, some new species had been described (e.g., Feijó et al., 2015; Rodríguez-Posada et al., 2021) or raised from junior synonymy (e.g., Rodríguez-Posada et al., 2021). Still the diversity of *Histiotus* is underestimated. There are two potential additions to the currently recognized diversity of the genus. The first might result from the revision of *Histiotus montanus*. *H. montanus* is the only species in the genus that is not monotypic, with two currently recognized subspecies: *H. m. montanus* and *H. m. inambarus* (Cláudio, 2019). The second potential addition is known from a single individual (*Histiotus* sp. 1–AMNH 268090) from the department of Cajamarca in Peru. This specimen was reported as distinct by Rodríguez-Posada et al. (2021) and therefore it represents a potential unnamed new species. After reviewing the specimen, we found several morphological characteristics (see comparisons section) that could grant it specific recognition. However, since it is only one specimen, it could be an outlier individual of *H. montanus*. Only its distinction in a phylogenetic analysis would warrant its description. Another issue that deserves attention is the population genetics of *H. macrotus* and *H. montanus*. The mean genetic distance between these two species is low (<1%, appendix 4), challenging their identity or suggesting the occurrence of local hybridization and introgression (Giménez et al., 2019).

Unlike most bat genera, only size and external characteristics exhibit intraspecific variation among all species in the genus. Craniodental characteristics in the genus are conserved and do not exhibit a clear variation among species.

Histiotus mochica increases the bat diversity of Peru to 192 species (Velazco, 2021), making it the third most diverse country with regard to bat species, behind Indonesia (233 spp.: Simmons and Cirranello, 2020) and Colombia (217 spp.: Rodríguez-Posada et al., 2021). *H. mochica* also becomes the 10th endemic bat species of the country (Velazco, 2021).

The knowledge and impact of indigenous communities to the conservation and gathering of natural history information on Neotropical fauna and flora has been the focus of several studies (e.g., Fleck et al., 2002; Cámara-Leret et al., 2019; Fernández-Llamazares et al., 2021). Herein we gave an example of a connection between an ancient pre-Incan civilization, the Moche, and a bat species previously unknown to science, but well known to the Moche (fig. 1). The highly stylized vase representing this bat species (fig. 1) attests to the heights reached by Moche artists; details captured in the piece, which allowed us to precisely identify this animal previously unknown to science, reveal their observation abilities, and unambiguously demonstrate their profound interest in nature. This highlights not only that the knowledge of present-day indigenous communities should be valued, but also that the knowledge of their ancient communities holds surprises that can enhance our knowledge of the natural world while strengthening our connection with the past.

Key to the Species of *Histiotus*

1. Transverse band of skin between pinnae absent, or <1 mm high; pinnae separated 2
1′. Transverse band of skin between pinnae present, and >1 mm high; pinnae joined 6
2. Transverse band of skin between pinnae absent 3
2′. Transverse band of skin between pinnae low, ~1 mm high 5
3. Ears <30 mm .... *H. magellanicus*
3′. Ears >30 mm 4
4. Ears triangular .... *H. cadenai*
4′. Ears oval or slightly triangular .... *H. colombiae*
5. General color dark; dorsal fur dark brown, and venter slightly paler than dorsum .... *H. alienus*
5′. General color light; dorsal fur golden brown, and ventral fur whitish .... *H. montanus*
6. Ears triangular; transverse band of skin between pinnae high, >3 mm 7
6′. Ears slightly triangular, transverse band of skin between pinnae low, <3 mm 9
7. Dorsal fur unicolored .... *H. mochica*
7′. Dorsal fur bicolored 8
8. Dorsal fur strongly bicolored, with well-marked bands; membranes translucent; ventral fur whitish .... *H. diaphanopterus*
8′. Dorsal fur weakly bicolored, with weakly marked bands; membranes light to dark brown; ventral fur light brown .... *H. velatus*
9. Ventral fur light brown/buff; facial profile of the skull sharply dished .... *H. humboldti*
9′. Ventral fur whitish; facial profile of the skull flat 10
10. Light colored membranes, translucent brown .... *H. laephotis*
10′. Dark colored membranes, brown/dark brown .... *H. macrotus*

ACKNOWLEDGMENTS

We are grateful to Richard Cadenillas, Oscar Centty, and Liz Huamaní for their assistance in the field. Many curators and support staff hosted visits, loaned specimens, and managed those loans, and we are grateful for their help: Adriano Lúcio Peracchi (ALP); Neil Duncan, Sara Ketelsen, Marisa Surovy, and Nancy Simmons (AMNH); Roberto Portela Miguez (BM); Erika Paliza (CEBIOMAS); Rubén Barquez and Mónica Díaz (CML); Bruce Patterson (FMNH); Jacob Esselstyn (LSUMZ); Pablo Teta (MACN); João Alves Oliveira (MN); Cecile Callou and Jean-Marc Pons (MNHN ZM-MO); and Darrin Lunde (USNM). Likewise, we are grateful to Emilio Bonifaz for reviewing and taking some measurements of the holotype and to Kerry Kline for her review of this manuscript. Field research was supported by the American Museum of Natural History Taxonomic Mammalogy Fund. This study was financed in part by the Coordenação de Aperfeiçoamento de Pessoal de Nível Superior–Brazil (CAPES) – Finance Code 001. Two anonymous reviewers read early drafts of this manuscript and made helpful suggestions for its improvement. The Cleveland Museum of Art kindly let us reproduce their photographs for figure 1.

REFERENCES

Affenzeller, S., H. Frauendorf, T. Licha, D.J. Jackson, and K. Wolkenstein. 2019. Quantitation of eumelanin and pheomelanin markers in diverse biological samples by HPLC-UV-MS following solid-phase extraction. PLoS ONE 14 (10): e0223552.

Alaica, A.K. 2020. Inverted worlds, nocturnal states and flying mammals: Bats and their symbolic meaning in Moche iconography. Arts 9: 107.

Amador, L.I., R.L. Moyers Arévalo, F.C. Almeida, S.A. Catalano, and N.P. Giannini. 2018. Bat systematics in the light of unconstrained analyses of a comprehensive molecular supermatrix. Journal of Mammalian Evolution 25: 37–70.

Aramayo, S.T., M.M. Díaz, M.D. Miotti, and E.J. Derlindati. 2019. First record of *Histiotus velatus* I. Geoffroy St.-Hilaire, 1824 (Chiroptera, Vespertilionidae) in Salta province, Argentina. Check List 15 (6): 973–978.

Baird, A.B., D.M. Hillis, J.C. Patton, and J.W. Bickham. 2008. Evolutionary history of the genus *Rhogeessa* (Chiroptera: Vespertilionidae) as revealed by mitochondrial DNA sequences. Journal of Mammalogy 89: 744–754.

Baird, A.B., M.R. Marchán-Rivadeneira, S.G. Pérez, and R.J. Baker. 2012. Morphological analysis and description of two new species of *Rhogeessa* (Chiroptera: Vespertilionidae) from the neotropics. Occasional Papers, Museum of Texas Tech University 307: 1–25.

Baird, A.B., et al. 2015. Molecular systematic revision of tree bats (Lasiurini): doubling the native mammals of the Hawaiian Islands. Journal of Mammalogy 96: 1255–1274.

Baird, A.B., et al. 2017. Nuclear and mtDNA phylogenetic analyses clarify the evolutionary history of two species of native Hawaiian bats and the taxonomy of Lasiurini (Mammalia: Chiroptera). PLoS ONE 12 (10): e0186085.

Baird, A.B., J.E. Light, and J.W. Bickham. 2019. A new species of *Rhogeessa* from Nicaragua based on morphological, karyotypic, and molecular data. *In* R.D. Bradley, H.H. Genoways, D.J. Schmidly, and L.C. Bradley (editors), From field to laboratory: a memorial volume in honor of Robert J. Baker: 257–273. Lubbock: Texas Tech University.

Baird, A.B., et al. 2021. On the utility of taxonomy to reflect biodiversity: the example of Lasiurini (Chiroptera: Vespertilionidae). Therya 12: 283–289.

Cámara-Leret, R., M.A. Fortuna, and J. Bascompte. 2019. Indigenous knowledge networks in the face of global change. PNAS 116: 9913–9918.

Castillo Butters L.J., and S. Uceda Castillo. 2008. The Mochicas. *In* H. Silverman and W.H. Isbell (editors), The handbook of South American archaeology: 707–729. New York: Springer.

Cláudio, V.C. 2019. Genus *Histiotus*. *In* D.E. Wilson and R.A. Mittermeier (editors), Handbook of the mammals of the world, vol. 9. Bats: 841–843. Barcelona: Lynx Editions.

Clement, M., D. Posada, and K.A. Crandall. 2000. TCS: a computer program to estimate gene genealogies. Molecular Ecology 9: 1657–1659.

Delhey, K. 2019. A review of Gloger's rule, an ecogeographical rule of colour: definitions, interpretations and evidence. Biological Reviews 94: 1294–1316.

Feijó, A., P.A. da Rocha, and S.L. Althoff. 2015. New species of *Histiotus* (Chiroptera: Vespertilionidae) from northeastern Brazil. Zootaxa 4048: 412–427.

Fernández-Llamazares, Á., et al. 2021. The importance of indigenous territories for conserving bat diversity across the Amazon basin. Perspectives in Ecology and Conservation 19: 10–20.

Fleck, D.W., R.S. Voss, and N.B. Simmons. 2002. Undifferentiated taxa and sublexical categorization: an example from Matses classification of bats. Journal of Ethnobiology 22: 61–102.

Gardner, A.L. 2008. Family Vespertilionidae Gray, 1821. *In* A.L. Gardner (editor), Mammals of South America, vol. 1: marsupials, xenarthrans, shrews, and bats: 440. Chicago: University of Chicago Press.

Giménez, A.L., N.P. Giannini, M.I. Schiaffini, and G.M. Martin. 2015. Geographic and potential distribution of a poorly known South American bat, *Histiotus macrotus* (Chiroptera: Vespertilionidae). Acta Chiropterologica 17: 143–158.

Giménez, A.L., N.P. Giannini, and F.C. Almeida. 2019. Mitochondrial genetic differentiation and phylogenetic relationships of three *Eptesicus* (*Histiotus*) species in a contact zone in Patagonia. Mastozoología Neotropical 26: 349–358.

Hammer, Ø., D.A.T. Harper, and P.D. Ryan. 2001. PAST: paleontological statistics software package for education and data analysis. Palaeontologia Electronica 4: 1–9.

Handley, C.O., Jr. 1996. New species of mammals from northern South America: Bats of the genera *Histiotus* Gervais and *Lasiurus* Gray (Chiroptera: Vespertilionidae). Proceedings of the Biological Society of Washington 109: 1–9.

Handley, C.O., Jr., and A.L. Gardner. 2008. Genus *Histiotus* P. Gervais, 1856. *In* A.L. Gardner (editor), Mammals of South America, vol. 1: Marsupials, xenarthrans, shrews, and bats: 450–457. Chicago: University of Chicago Press.

Hoofer, S.R., and R.A. Van Den Bussche. 2003. Molecular phylogenetics of the chiropteran family Vespertilionidae. Acta Chiropterologica 5: 1–63.

Koopman, K.P. 1982. Biogeography of the bats of South America. *In* M.A. Mares and H. H. Genoways (editors), Mammalian biology in South America: 273–302. Pittsburgh: University of Pittsburgh.

Koopman, K.F. 1994. Chiroptera: systematics. Handbuch der Zoologie VIII (Mammalia) 60: 1–217.

Larco Hoyle, R. 2001. Los Mochicas, vol. 1. Lima: Museo Arqueológico Rafael Larco Herrera.

Larsen, R.J., et al. 2012. Genetic diversity of Neotropical *Myotis* (Chiroptera: Vespertilionidae) with an emphasis on South American species. PLoS ONE 7 (10): e46578.

Leigh, J.W., and D. Bryant. 2015. POPART: full-feature software for haplotype network construction. Methods in Ecology and Evolution 6: 1110–1116.

Ludeña, J.P., and C.E. Medina. 2017. Segundo registro de *Cyttarops alecto* y *Eumops wilsoni* (Mammalia: Chiroptera) en el Perú. Revista Peruana de Biologia 24: 401–406.

Miller, G.S., Jr. 1907. The families and genera of bats. Bulletin of the United States National Museum 57: i–xvii, 1–282, 14 pls.

Moratelli, R., A.L. Peracchi, and J.A. de Oliveira. 2011a. Morphometric and morphological variation in *Myotis simus* Thomas (Chiroptera, Vespertilionidae), with an appraisal of the identity of *Myotis guaycuru* Proença based on the analysis of the type material. Zootaxa 2985: 41–54.

Moratelli, R., A.L. Peracchi, D. Dias, and J.A. de Oliveira. 2011b. Geographic variation in South American populations of *Myotis nigricans* (Chiroptera, Vespertilionidae), with the description of two new species. Mammalian Biology 76: 592–607.

Moratelli, R., A.L. Gardner, J.A. de Oliveira, and D.E. Wilson. 2013. Review of *Myotis* (Chiroptera, Vespertilionidae) from northern South America, including description of a new species. American Museum Novitates 3780: 1–36.

Moratelli, R., et al. 2019a. Family Vespertilionidae. *In* D.E. Wilson and R.A. Mittermeier, (editors), Handbook of the mammals of the world, vol. 9. Bats: 716–759. Barcelona: Lynx Editions.

Moratelli, R., R.L.M. Novaes, C. Carrión Bonilla, and D.E. Wilson. 2019b. A new species of *Myotis* (Chiroptera, Vespertilionidae) from Peru. *In* R.D. Bradley, H.H. Genoways, D.J. Schmidly, and L.C. Bradley (editors), From field to laboratory: a memorial volume in honor of Robert J. Baker: 239–256. Lubbock: Texas Tech University.

Ossa, G., H.T. Zamora, and P.M. Velazco. 2020. *Platalina genovensium* (Chiroptera: Phyllostomidae). Mammalian Species 52 (995): 105–113.

Piaggio, A.J., and S.L. Perkins. 2005. Molecular phylogeny of North American long-eared bats (Vespertilionidae: *Corynorhinus*); inter- and intraspecific relationships inferred from mitochondrial and nuclear DNA sequences. Molecular Phylogenetics and Evolution 37: 762–775.

Reid, F. 2009. A field guide to the mammals of Central America and southeast Mexico. New York: Oxford University Press.

Rensch, B. 1929. Das Prinzip geographischer Rassenkreise und das Problem der Artbildung. Berlin: Gebrueder Borntraeger.

Rensch, B. 1936. Some problems of geographical variation and species-formation. Proceedings of the Linnean Society of London 150: 275–285.

Rodríguez-Posada, M.E., D.M. Morales-Martínez, H.E. Ramírez-Chaves, D. Martínez-Medina, and C.A. Calderón-Acevedo. 2021. A new species of long-eared brown bat of the genus *Histiotus* (Chiroptera) and the revalidation of *Histiotus colombiae*. Caldasia 43: 221–234.

Roehrs, Z.P., J.B. Lack, and R.A. Van Den Bussche. 2010. Tribal phylogenetic relationships within Vespertilioninae (Chiroptera: Vespertilionidae) based on mitochondrial and nuclear sequence data. Journal of Mammalogy 91: 1073–1092.

Ruedi, M., and F. Mayer. 2001. Molecular systematics of bats of the genus *Myotis* (Vespertilionidae) suggests deterministic ecomorphological convergences. Molecular Phylogenetics and Evolution 21: 436–448.

Semedo, T.B.F., and A. Feijó. 2017. Filling the gap: first record of the transparent-winged big-eared bat *Histiotus diaphanopterus* (Chiroptera: Vespertilionidae) in southwestern Brazil. Mammalia 81: 323–327.

Simmons, N.B. 2005. Order Chiroptera. *In* D.E. Wilson and D.M. Reeder (editors), Mammal species of the world, a taxonomic and geographic reference, 3rd ed.: 312–529. Baltimore: Johns Hopkins University Press.

Simmons, N.B., and A.L. Cirranello. 2020. Bat species of the world: a taxonomic and geographic database. Online resource (https://batnames.org), accessed on June 3, 2021.

Stecher, G., K. Tamura, and S. Kumar. 2020. Molecular Evolutionary Genetics Analysis (MEGA) for macOS. Molecular Biology and Evolution 37: 1237–1239.

Templeton, A.R., K.A. Crandall, and C.F. Sing. 1992. A cladistic analysis of phenotypic associations with haplotypes inferred from restriction endonuclease mapping and DNA sequence data. III. Cladogram estimation. Genetics 132: 619–633.

Thomas, O. 1916. Notes on bats of the genus *Histiotus*. Annals and Magazine of Natural History (ser. 8) 17: 272–276.

Velazco, P.M. 2021. Murciélagos del Perú/Bats of Peru. Online resource (http://www.paulvelazco.com/murcielagos_peru.html), accessed June 3, 2021.

Velazco, P.M., and K.A. Kline. 2019. *Tomopeas ravus* (Chiroptera: Molossidae). Mammalian Species 51 (979): 70–74.

Velazco, P.M., R. Cadenillas, O. Centty, L. Huamaní, and H. Zamora. 2013. New records of *Platalina genovensium* Thomas, 1928 (Chiroptera, Phyllostomidae, Lonchophyllinae) and *Tomopeas ravus* Miller, 1900 (Chiroptera, Molossidae, Tomopeatinae). Mastozoología Neotropical 20: 425–434.

Velazco, P.M., A.G. Autino, and G.L. Claps. 2014. New record of the ectoparasite insect *Speiseria ambigua* Kessel, 1925 (Diptera: Streblidae) of *Platalina genovensium* Thomas, 1928 (Chiroptera: Phyllostomidae) from Peru. Check List 10: 1525–1527.

Ziegler, A.C., F.G. Howarth, and N.B. Simmons. 2016. A second endemic land mammal for the Hawaiian Islands: a new genus and species of fossil bat (Chiroptera: Vespertilionidae). American Museum Novitates 3854: 1–52.

APPENDIX 1

Specimens Examined

The following list includes all specimens of *Histiotus* used in the morphological components of this study with data on their respective localities. See Material and Methods for abbreviations. Specimens used in the morphometric analyses are marked with an asterisk.

H. alienus (*N = 1*). BRAZIL: *Santa Catarina* (BM 1909.11.19.1* [holotype of *Histiotus alienus*]).

H. cadenai (*N = 1*). ECUADOR: *Tungurahua*: Patate, San Francisco, E of Ambato (AMNH 67648*).

H. colombiae (*N = 14*). COLOMBIA: *Cundinamarca*: Bogotá (FMNH 72165–72166, 72167–72168*, 72169, 72170–72171*, 72172–72174); Choachí (BM 1899.11.4.1 [holotype of *Histiotus colombiae*]). ECUADOR: *Pichincha*: Quito (MNHN-ZM-MO 1904-1179). *Tungurahua*: 1.5 km E of Mirador (USNM 513495–513496*).

H. diaphanopterus (*N = 1*). BOLIVIA: *Santa Cruz*: Valle Grande, 5.5 km NE of Valle Grande (AMNH 264086*).

H. humboldti (*N = 4*). VENEZUELA: *Amazonas*: Cerro Neblina, Camp II, 2.8 km NE Pico Phelps (=Neblina) (USNM 560627*). *Distrito Capital*: Caracas, Los Venados, 4 Km NNW of Caracas (USNM 370967*); Caracas, Pico Ávila, 5 Km NNE Caracas, near Hotel Humboldt (USNM 370970*). *Mérida*: Montes de la Hechicera (MNHN-ZM-MO 1972-762*).

H. laephotis (*N = 18*). ARGENTINA: *Catamarca*: Cuesta del Clavillo (CML 5253*); Paclin (CML 10833*). *Jujuy*: Cueva del Tigre, El Milagro (MACN 16811); Ledesma, Yuto (AMNH 181527, 181528*); San Pedro (CML 7058*). *Salta*: (BM 1934.11.4.1, 1934.11.4.2); La Viña, La Viña, Iglesia (MACN 16810). *Tucumán*: (BM 1904.10.2.1*); Burruyacú, El Naranjo (MACN 16814); Horco Molle (CML 4515*); Yerba Buena (CML 6103*); San Miguel de Tucumán (BM 1902.1.5.1*). BOLIVIA: *Cochabamba*: (BM 1934.9.2.20). *Potosí*: Caiza (BM 1897.2.25.1* [holotype of *Histiotus laephotis*], BM 1897.2.25.4*). PERU: *Huancavelica*: (BM 1938.9.26.3*).

H. macrotus (*N = 21*). ARGENTINA: *Catamarca*: Dique El Potrero (CML 6061*); 5km NW of Chumbicha (CML 7894*). *Neuquén*: P.N. Huapi (CML 9884*). *Río Negro*: El Bolson (LSUMZ 16784*). *Salta*: 20km N of Cafayate (CML 5406*). *Tucumán*: Chicligasta (CML 6185*); Pueblo Viejo (CML 6059). CHILE: (MNHN-ZM-MO 1999-962). *Región Metropolitana de Santiago*: Santiago (BM 1935.11.10.1*, 1935.11.10.3*, 1935.11.10.4, 1935.11.10.5*, 1935.11.10.6*, 1935.11.10.13*, 1935.11.10.14*, 1935.11.10.16*, 1935.11.10.17*, 1935.11.10.18*, 1935.11.10.19; USNM 391787–391788).

H. magellanicus (*N = 17*). ARGENTINA: *Neuquén*: (CML 3231*); Los Lagos (CML 10853–10854*); Parque Nacional Nahuel Huapi (CML 9887*). CHILE: *Región de Aysén del General Carlos Ibáñez del Campo*: Aysén, Almirante Simpson, Isla Gran Guaiteca (FMNH 127477–127480*). *Región de La Araucanía*: (BM 1908.3.1.1*); Cautin Lake Gualletue (FMNH 23624*); Malleco, Angol (AMNH 93314*); Malleco, Curacautin (FMNH 23622, 23623*). *Región de Los Lagos*: Chiloé, Río Inio (FMNH 23619*, 23620); Valdivia, Mafil, 20 mi SW of Valdivia (FMNH 23621*). *Región de Magallanes y de la Antártica Chilena*: Last Hope Inlet (BM 1907.4.5.1).

H. mochica (*N = 2*). PERU: *Piura*: Talara, Quebrada Pariñas, 9.6 km NE of Talara (AMNH 278521*; CEBIOMAS 227* [holotype of *Histiotus mochica*]).

H. montanus (*N = 27*). ARGENTINA: *Catamarca*: Las Estancias (CML 1758). *Chubut*: (BM 1928.12.11.1*); Cushamen, Río Turbio (MACN 16505). *Córdoba*: (BM 1916.1.6.1*, 1916.1.6.2*). *Neuquén*: Catan, Las Coloradas (MACN 13844). *Río Negro*: Bariloche, La Paloma, 4 km SE de San Carlos de Bariloche (MACN 23650). *San Juan*: Jachal (CML 5568*). *San Luis*: Coronel Pringles, Río Quinto, Santa Inés (MACN 16809). *Tucumán*: (BM 1904.10.2.2*); Burruyacú, Anta Mapu (MACN 16813*); Burruyacú, El Naranjo (MACN 16815*). CHILE: (MNHN-ZM-MO 1874-53). *Región Metropolitana de Santiago*: Santiago, Puente Alto (BM 1903.7.3.2*). *Región de Valparaíso*: Zapallar (USNM 391789*). PERU: *Arequipa*: Islay, Chucarapi (FMNH 50780, 50781*). *Cuzco*: ca 14 km NE Abra Malaga on Ollantaytambo-Quillabamba Rd (LSUMZ 19215*). *Huancavelica*: Angaraes, Lircay (FMNH 75149). *Puno*: Inambari River (AMNH 37194 [holotype of *Histiotus inambarus*]). *San Martín*: Puerta del Monte, ca 30 km NE Los Alisos (LSUMZ 27260*). URUGUAY: *Canelones*: Jaureguiberry Beach (AMNH 188780*). *Flores*: Ciudad de Trinidad (AMNH 188781*). *Rivera*: Rivera (FMNH 65634–65635*). *San José*: Chamizo, Estancia Santa Clara (AMNH 183876*; USNM 548682*).

Histiotus sp. 1 (*N = 1*). PERU: *Cajamarca*: Celendín, Las Ashitas, 4 kilometers west of Pachapiriana (AMNH 268090*).

H. velatus (*N = 44*). ARGENTINA: *Corrientes*: Santo Tomé, Gobernador Ingeniero Valentín Virasoro (MACN 18055*). *Misiones*: Oberá, Oberá (MACN 18053–18054*); Oberá, Campo Ramón (MACN 18056–18059). BRAZIL: *Maranhão*: Tranqueira (FMNH 26466). *Mato Grosso*: Chapada, Santa Anna de Chapada (BM 1903.7.7.17* [holotype of *Histiotus velatus miotis*]). *Minas Gerais*: Lagoa Santa (MN 6516); Viçosa (USNM 391142*, 548683–548684*). *Rio de Janeiro*: Ilha Grande (MN 23071*); Ilha Grande (MN 23072); Itaguaí, Rural (MACN 16812); Itaguaí, Universidade Federal Rural de Rio de Janeiro (ALP 1522*, 1579*, 1581*, 2096*, 2349*, 2350*, 4845*, 4942*, 5088*); Itaguaí, Universidade Federal Rural de Rio de Janeiro, Jardim botânico (ALP 5595*); Rio de Janeiro, Quinta da Boa Vista (MN 3547*, 23049*). Sainte Tereza (MNHN-ZM-MO 1999-963). PARAGUAY: *Distrito Capital*: Asunción, Colonia Asunción (MACN 16808). *Guairá*: Villarrica (AMNH 243887; USNM 105589); Villarrica, Caroveny (AMNH 217565). PERU: *Cuzco*: Quispicanchi, Hacienda Cadena (FMNH 66389, 66391*, 66393*, 68496*, 68504, 68506*); Quispicanchi, Quincemil (FMNH 68497–68499*, 68501–68502*).

APPENDIX 2

Vector Correlation Coefficients

Vector correlation coefficients between original variables and principal components (PC1 and PC2) and between original variables and canonical variates (DF1 and DF2) for species of *Histiotus*. See Material and Methods for definitions and abbreviations of variables.

Measurements	PC 1	PC 2	DF1	DF2
F	0.100	0.149	0.001	-0.001
CIL	0.209	-0.132	0.003	-0.005
CCL	0.217	-0.122	0.004	-0.005
PB	0.275	0.863	0.010	0.009
ZB	0.365	-0.150	0.008	-0.007
BB	0.201	0.256	0.006	0.001
MB	0.245	0.011	0.005	-0.002
MTL	0.372	-0.100	0.009	-0.006
BAM	0.371	-0.012	0.009	-0.005
UPTL	0.328	-0.061	0.008	-0.007
DENL	0.286	-0.264	0.005	-0.008
MANDL	0.353	-0.169	0.008	-0.007
Proportion of variance (%)	69.73	13.82	58.71	19.17

APPENDIX 3

Confusion Matrix

Confusion matrix of *Histiotus* species inferred from discriminant function analysis (DFA) assigning individuals to one of the 12 taxa based on the analysis of one external and 11 craniodental characters.

Species	1	2	3	4	5	6	7	8	9	10	11	12	Total	% correctly classified[1]
1-*H. alienus*	**1**	0	0	0	0	0	0	0	0	0	0	0	1	100%
2-*H. cadenai*	0	**1**	0	0	0	0	0	0	0	0	0	0	1	100%
3-*H. colombiae*	0	0	**5**	0	0	0	0	1	0	0	0	0	6	83.3%
4-*H. diaphanopterus*	0	0	0	**1**	0	0	0	0	0	0	0	0	1	100%
5-*H. humboldti*	0	0	0	0	**4**	0	0	0	0	0	0	0	4	100%
6-*H. laephotis*	0	1	0	0	0	**5**	0	0	1	1	3	0	11	45.5%
7-*H. macrotus*	0	0	0	0	0	1	**11**	2	0	1	0	0	15	73.3%
8-*H. magellanicus*	0	0	1	0	0	0	1	**11**	0	1	0	0	14	78.6%
9-*H. mochica*	0	0	0	0	0	0	0	0	**2**	0	0	0	2	100%
10-*H. montanus*	1	1	1	0	0	0	1	1	0	**13**	0	0	18	72.2%
11-*H. velatus*	0	1	0	0	0	3	0	0	0	1	**24**	0	29	82.8%
12-*Histiotus* sp. 1	0	0	0	0	0	0	0	0	0	0	0	**1**	1	100%
Total	2	4	7	1	4	9	13	15	3	17	27	1	103	

[1] Percentage of individuals correctly classified by the DFA.

APPENDIX 4

Matrix of Genetic Distances

Pairwise uncorrected (*p*) percentage of cyt-*b* sequence divergence (x̄ ± SD) within and among *Histiotus* species. All sequences were cropped to 767 bp of the mitochondrial cyt-*b* gene.

	1	2	3	4	5	6
1–*Histiotus colombiae*	0.85 ± 0.61					
2–*Histiotus humboldti*	12.55 ± 0.53	1.09 ± 0.56				
3–*Histiotus macrotus*	12.75 ± 0.19	5.93 ± 0.29	0.22 ± 0.16			
4–*Histiotus magellanicus*	11.20 ± 0.12	10.62 ± 0.53	11.25 ± 0.15	0.22 ± 0.16		
5–*Histiotus mochica*	11.66 ± 0.18	3.20 ± 0.29	6.27 ± 0.17	10.00 ± 0.15	0	
6–*Histiotus montanus*	12.74 ± 0.19	5.87 ± 0.25	0.20 ± 0.18	11.23 ± 0.14	6.21 ± 0.07	0.09 ± 0.07

All issues of *Novitates* and *Bulletin* are available on the web (http://digitallibrary.amnh.org/dspace). Order printed copies on the web from:
http://shop.amnh.org/a701/shop-by-category/books/scientific-publications.html

or via standard mail from:

American Museum of Natural History—Scientific Publications
Central Park West at 79th Street
New York, NY 10024

♾ This paper meets the requirements of ANSI/NISO Z39.48-1992 (permanence of paper).